

# Response to Reviewer Comments

Manuscript: “Efficient Uzawa algorithms with projection strategies  
for geodynamic Stokes flow”

by Jang, Lee, Thieulot, Choi and So

Dear Editor and Professor Schmalholz,

We sincerely thank Professor Schmalholz for the positive and constructive review of our manuscript. We appreciate the recognition that the manuscript is clearly structured and of interest for readers developing numerical algorithms for geodynamic processes. The helpful comments and suggestions have further improved the manuscript. Below, we provide detailed point-by-point responses to all comments and describe the corresponding changes made to the revised manuscript. All modifications will be highlighted in green in the revised manuscript.

## Main Comment

### 3D benchmark comparison

**Reviewer:** *The authors motivate their work in line 18 with 3D problems which indeed represent a major challenge. However, the authors do not show the computational performance and advantage of their new algorithm for 3D problems (except the ABC Flow). The presented examples are useful, but I think a 3D example, for example a simple 3D thermal convection or subduction scenario, would increase the relevance of the presented algorithms. One could show results of a 3D simulation done with a “standard” solver and compare it to the results of a 3D simulation done with the solver presented in the manuscript. Such comparison could maybe better show the advantage and potential computational gain of the solver presented. But this is just a suggestion.*

### Response:

We thank the reviewer for this constructive suggestion. Following this recommendation, we have added a three-dimensional thermochemical convection benchmark in Appendix C. The problem extends the two-dimensional configuration of Section 3.4 to three dimensions by adding a unit-depth lateral dimension, using the same boundary-layer initial temperature field, basal dense layer, and temperature-dependent viscosity. The domain  $[0, 2] \times [0, 1] \times [0, 1]$  was discretized with a  $100 \times 50 \times 50$  structured tetrahedral mesh using Mini elements (P1+Bubble/P1), which satisfy the LBB stability condition and thus provide an independent verification that the CD-U- $\eta$  algorithm operates correctly with a different stable element pair than the Taylor-Hood elements used in the two-dimensional benchmarks. The transport equations for temperature and composition were discretized with P1 discontinuous Galerkin elements using upwind fluxes and advanced in time with the second-order BDF2 scheme, which ensures stable advection without requiring additional stabilization. Since the purpose of this three-dimensional test is to verify the algorithmic behavior of CD-U- $\eta$  and the projection post-processing rather than to assess solution accuracy, we adopted a fixed time step of  $\Delta t = 10^{-5}$  and advanced the solution to the same target time  $t = 5 \times 10^{-3}$  as in the two-dimensional configuration.

Since a direct solver reference solution is not feasible at this mesh resolution in three dimensions, the comparison focuses on the effect of the projection strategy rather than on accuracy relative to a reference. The Stokes system was solved at each time step using CD-U- $\eta$  with and without the

projection post-processing, and convergence was monitored through the normalized weak divergence residual  $R_{\text{div}}$ . The results show that the projection consistently reduces  $R_{\text{div}}$  across all time steps, confirming that the effectiveness of the projection post-processing observed in the two-dimensional benchmarks carries over to three-dimensional problems.

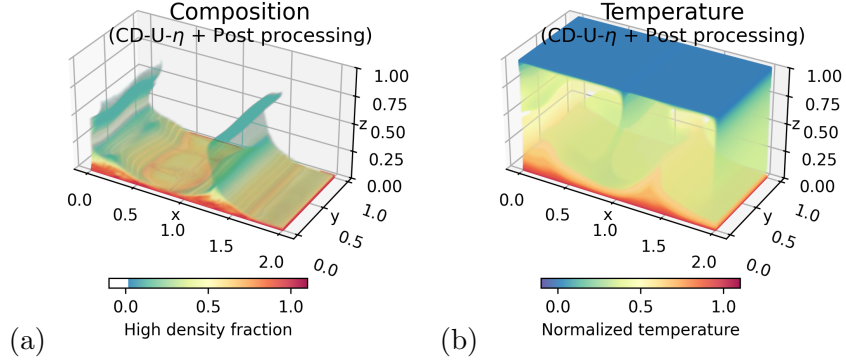


Figure 1: Three-dimensional thermochemical convection at  $t = 5 \times 10^{-3}$  solved with CD-U- $\eta$  + projection on a  $100 \times 50 \times 50$  Mini element mesh. (a) Composition field showing entrainment of the basal dense layer. (b) Normalized temperature field.

Figure 1 shows the temperature and composition fields at  $t = 5 \times 10^{-3}$ , where thermal plumes and entrainment of the basal dense layer are consistent with the two-dimensional results.

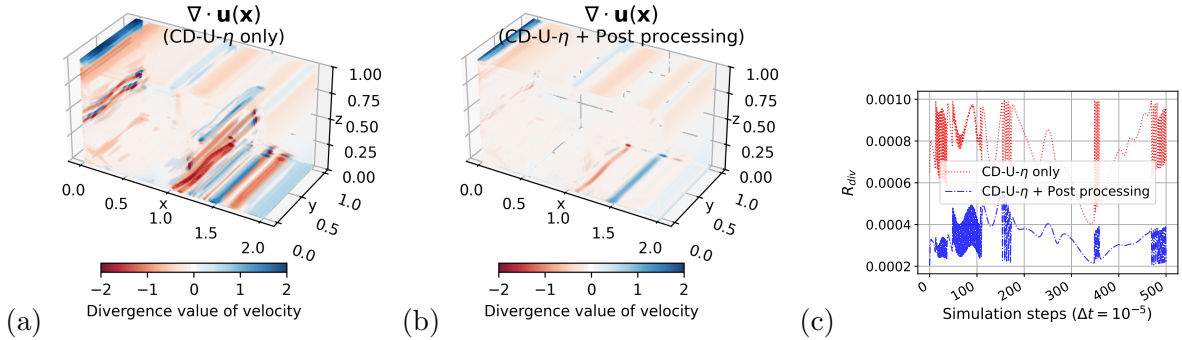


Figure 2: Spatial distribution of  $\nabla \cdot \mathbf{u}$  at  $t = 5 \times 10^{-3}$  for (a) CD-U- $\eta$  only and (b) CD-U- $\eta$  + projection. (c) Evolution of the normalized weak divergence residual  $R_{\text{div}}$  over 501 time steps for CD-U- $\eta$  only and CD-U- $\eta$  + projection.

Figure 2(a) and (b) show that the projection markedly suppresses the divergence error throughout the domain, with the localized concentrations near the plume regions in (a) largely eliminated in (b). The  $R_{\text{div}}$  history in Figure 2(c) confirms that this reduction is maintained consistently across all time steps, with the projection lowering  $R_{\text{div}}$  by approximately a factor of two, consistent with the two-dimensional results.

### Changes in manuscript:

Added Appendix C presenting the three-dimensional thermochemical convection benchmark, including the problem setup, convergence history of  $R_{\text{div}}$  with and without projection, solution snapshots, and the spatial distribution of  $\nabla \cdot \mathbf{u}$  at the final time step.

## Minor Comments

### Comment 1: Subplot labels and captions

**Reviewer:** *General: Subplots in the figures should be labeled (e.g. a), b) etc.) and the captions could be improved to better explain the figures.*

#### Response:

We thank the reviewer for this suggestion. All figures have been updated with subplot labels (a), (b), etc., and the captions have been revised to provide more detailed descriptions of the quantities shown, including mesh resolution and element type where applicable.

#### Changes in manuscript:

Subplot labels and improved captions added to all figures (Figures 1–8).

### Comment 2: Algorithm presentation

**Reviewer:** *General: Maybe flowcharts could help to explain the algorithms presented in sections 2.2 and 2.3.*

#### Response:

We thank the reviewer for this suggestion. Since the mathematical formulations are central to the algorithms and the iterations are purely sequential without branching, we opted for structured summary boxes rather than flowcharts. Each box presents the algorithmic steps with descriptive labels alongside the full variational forms, which we believe conveys the sequential structure clearly while preserving the mathematical detail that would be difficult to accommodate in a flowchart format. As an example, the CD-U- $\eta$  algorithm box is shown below.

#### CD-U- $\eta$

*Initialization:* Set  $p^0 = 0$

*Initial solve:* Find  $u^1$  satisfying  $Ku^1 = f - Gp^0$

*Initial residual:* Find  $q^1$  satisfying  $\langle q^1, r \rangle = \langle h + \nabla \cdot u^1, r \rangle \quad \forall r \in Q$

*Preconditioning:* Find  $w^1$  satisfying  $\langle \frac{1}{\eta} w^1, r \rangle = \langle q^1, r \rangle \quad \forall r \in Q$ , set  $d^1 = -w^1$

*Iteration ( $k \geq 1$ ):*

*Direction solve:* Find  $z^k$  satisfying  $Kz^k = Gd^k$

*Step-size selection:* Compute  $\alpha_k = \langle q^k, w^k \rangle / \langle \nabla d^k, z^k \rangle$

*Pressure update:* Compute  $p^{k+1} = p^k + \alpha_k d^k$

*Velocity update:* Compute  $u^{k+1} = u^k - \alpha_k z^k$

*Residual update:* Find  $q^{k+1}$  satisfying  $\langle q^{k+1}, r \rangle = \langle h + \nabla \cdot u^{k+1}, r \rangle \quad \forall r \in Q$

*Preconditioning:* Find  $w^{k+1}$  satisfying  $\langle \frac{1}{\eta} w^{k+1}, r \rangle = \langle q^{k+1}, r \rangle \quad \forall r \in Q$

*Conjugate direction:* Compute  $\beta_k = \langle q^{k+1}, w^{k+1} \rangle / \langle q^k, w^k \rangle$ , set  $d^{k+1} = -w^{k+1} + \beta_k d^k$

#### Changes in manuscript:

Structured algorithm boxes added for the Standard Uzawa, Adaptive Uzawa, CD-U, CD-U- $\eta$ , and projection post-processing in Sections 2.2 and 2.3.

**Comment 3: Line 12 – High viscosity value**

**Reviewer:** *Maybe provide a value of what you consider as high viscosity.*

**Response:**

We have specified a representative range of mantle viscosity ( $10^{19}$ – $10^{23}$  Pa s) in the revised text.

**Changes in manuscript:**

Line 12: “The mantle has high viscosity” replaced with “The mantle has a viscosity on the order of  $10^{19}$ – $10^{23}$  Pa s.”

**Comment 4: Line 150 – Equation numbering**

**Reviewer:** *Equations are not numbered anymore.*

**Response:**

In our manuscript, we follow the convention that only equations cross-referenced elsewhere in the text receive numbers. Display equations that are self-contained within their local context are left unnumbered. In the revised manuscript, we applied this convention consistently: equations that carried numbers but were never referenced have been changed to unnumbered display equations. In addition, the algorithm presentations in Sections 2.2 and 2.3 have been restructured into summary boxes (see our response to Comment 2), which removed some previously numbered equations. Cross-references that pointed to equations now contained in algorithm boxes have been replaced with descriptive references to the corresponding boxes.

**Changes in manuscript:**

Unreferenced numbered equations have been changed to unnumbered form, and cross-references that pointed to equations now contained in algorithm boxes have been replaced with descriptive references to the corresponding boxes (e.g., “CD-U algorithm box in Section 2.2”).

**Comment 5: Line 198 – Strong viscosity contrast**

**Reviewer:** *Please specify what is a strong viscosity contrast, for example four orders of magnitude or similar.*

**Response:**

We agree that the original phrasing was vague. The viscosity contrasts used in our benchmarks are:  $10^6$  for SolCx (Section 3.3.2),  $10^6$  for SolKz (Appendix A),  $10^2$ – $10^{10}$  for the multisinker problem (Section 3.3.3), and  $10^3$  for the block sinking problem (Section 3.4.2). We have revised the sentence to remove the unspecified claim, since the concrete values are already stated in each benchmark section.

**Changes in manuscript:**

Line 198: “strong viscosity contrasts and heterogeneous distributions” replaced with “across the benchmark problems considered here.”

### Comment 6: Line 203 – Typical tolerances

**Reviewer:** *“These tolerances are stricter than typical values in geodynamic simulations.” Please provide references for this statement and provide a number for “typical values”.*

#### Response:

We thank the reviewer for pointing this out. The tolerances  $10^{-10}$  (relative) and  $10^{-12}$  (absolute) refer to the inner linear solves within each Uzawa iteration. Our intent was to make these inner solves effectively exact so that the convergence behavior observed in our benchmarks is determined by the outer Uzawa iteration alone, not by inner solver errors. We have revised the text to clarify this rationale. For reference, the ASPECT code (Kronbichler et al., 2012) uses default inner solve tolerances of  $10^{-2}$  for the velocity block and  $10^{-6}$  for the Schur complement block.

#### Changes in manuscript:

Revised the sentence on inner solver tolerances to clarify the rationale and added the ASPECT solver parameters as a reference point (Kronbichler et al., 2012).

### Comment 7: Figure 1 – Numerical resolution

**Reviewer:** *What was the numerical resolution?*

#### Response:

We thank the reviewer for noting this omission. The ABC flow benchmark in Figure 1 was computed on a  $32 \times 32 \times 32$  structured tetrahedral mesh with P2-P1 Taylor-Hood elements. This information has been added to the figure caption.

#### Changes in manuscript:

Figure 1 caption revised to include the mesh resolution and element type (see also Comment 1).

### Comment 8: Line 283 – Constant $\kappa$

**Reviewer:** *If  $\kappa$  is constant you could bring it out of the spatial derivative, since it should also include density and specific heat.*

#### Response:

We thank the reviewer for this remark. We have clarified that  $\kappa$  denotes the thermal diffusivity, defined as  $\kappa = k/(\rho c_p)$  where  $k$  is the thermal conductivity,  $\rho$  the density, and  $c_p$  the specific heat capacity. In the nondimensional formulation used for this benchmark,  $\kappa$  is set to unity.

#### Changes in manuscript:

Clarified the definition of  $\kappa$  as thermal diffusivity with its explicit form  $\kappa = k/(\rho c_p)$ , and noted the nondimensional setting  $\kappa = 1$ .

### Comment 9: Figure 6 – Caption

**Reviewer:** *The caption should state what simulation the figures shows; the block sinking problem.*

#### Response:

We have revised the caption to explicitly state that Figure 6 shows the block sinking benchmark (see also Comment 1).

**Changes in manuscript:**

Figure 6 caption revised to include “Block sinking benchmark” (see Comment 1).